Asociación Argentina
de Mecánica Computacional

Mecánica Computacional Vol XLII, pp. 321-330
A. Caggiano, G. Etse, P. Folino, M. Goldschmit, M. Pucheta, M. Storti (Eds.)
J. Ballaben, D. Felix, R. Jaca (Issue eds.)
Buenos Aires, November 11-14, 2025

DYNAMIC BEHAVIOR OF TRANSMISSION CONDUCTORS UNDER RUPTURE CONDITIONS THROUGH FINITE ELEMENT MODELING

Ariel G. Terlisky[a,b], Jodie A. Crocker[a], Jorge G. Laiun[a,b] and David Folk[c]

[a]*SRK Consulting Argentina. Chile 300, 1098 Ciudad Autónoma de Buenos Aires, Argentina, aterlisky@srk.com.ar, https://www.srk.com/es/*

[b]*Facultad de Ingeniería, Universidad de Buenos Aires, Av. Las Heras 2214, 1127 Ciudad Autónoma de Buenos Aires, Argentina, aterlisky@fi.uba.ar, https://www.fi.uba.ar/*

[c]*Electrical Power Research Institute (EPRI), 3420 Hillview Avenue, Palo Alto, CA 94304, https://www.epri.com/*

Keywords: Transmission conductors, Rupture, Dynamic Analysis, ADINA.

Abstract. Understanding the dynamic behavior of transmission conductors under rupture conditions is a critical factor in ensuring the reliability and safety of power transmission systems. This is commonly studied by analyzing the dynamic load factor (DLF), which is a measure of the loads experienced by the system. This study investigates the impact of conductor properties on DLF through extensive finite element modeling and sensitivity analyses using the ADINA software by Bentley Studios. These finite element models carefully consider both internal (i.e. axial and lateral) and aerodynamic damping in the form of damping parameters, as these greatly influence the dynamic behavior of the models. Initially, simple models with a single conductor span were analyzed to understand the effects of span length, conductor stiffness, and catenary constants on DLF. Two examples are shown, which mimic full-scale tests conducted at the Dynamic Impact Test Line at the EPRI High Voltage Laboratory. After calibrating the FEM modeling parameters, the FEM results show high agreement with the full-scale test results. Following additional tests, a comparison of DLF vs. suspension structure stiffness is made, which indicates that higher suspension structure stiffness generally increases the DLF of both suspension and strain structures with less impact at higher stiffnesses. Subsequently, the scope was expanded to include multi-span configurations containing multiple suspension structures. An example is shown where the number of suspension structures ranges from 1 to 20. These results indicate that the effect of multiple suspension structures on DLF is complicated, likely due to the reflection of shockwaves between structures. This study provides valuable insight into the relationship between broken conductors and the resulting transmission line behavior, allowing engineers to mitigate risks when designing power transmission networks.

ISSN: 2591-3522 DOI: 10.70567/mc.v42.ocsid8223

1 INTRODUCTION

High voltage transmission lines are a critical component of modern infrastructure, serving as the conduit for large-scale electrical energy transfer. One way to enhance the resiliency of transmission lines is designing for broken conductor events. These events, while rare, may cause severe mechanical instability in a transmission line, in some cases leading to structure failures propagating 30 km or more. By designing for broken wire events, structures can be properly reinforced to handle the resulting instability, containing the damage and leading to reduced power restoration times.

When a transmission line conductor ruptures, an instantaneous shock load is generated and transmitted along the conductor axis at the speed of sound in the material, which for metallic conductors is approximately 4500 m/s. This axial shockwave can be reflected at the end of a tension section, potentially impacting strain structures located some distance from the initial rupture point. Such behavior was verified in full-scale testing and numerical simulations, notably by Vicent Pierre (2004), who investigated multiple failure modes—including insulator string, conductor, ground wire, and tower failures—and demonstrated that the ADINA (2024) software is capable of accurately reproducing these complex dynamic phenomena. An example load at a suspension and strain support following a broken wire event is shown in Figure 1.

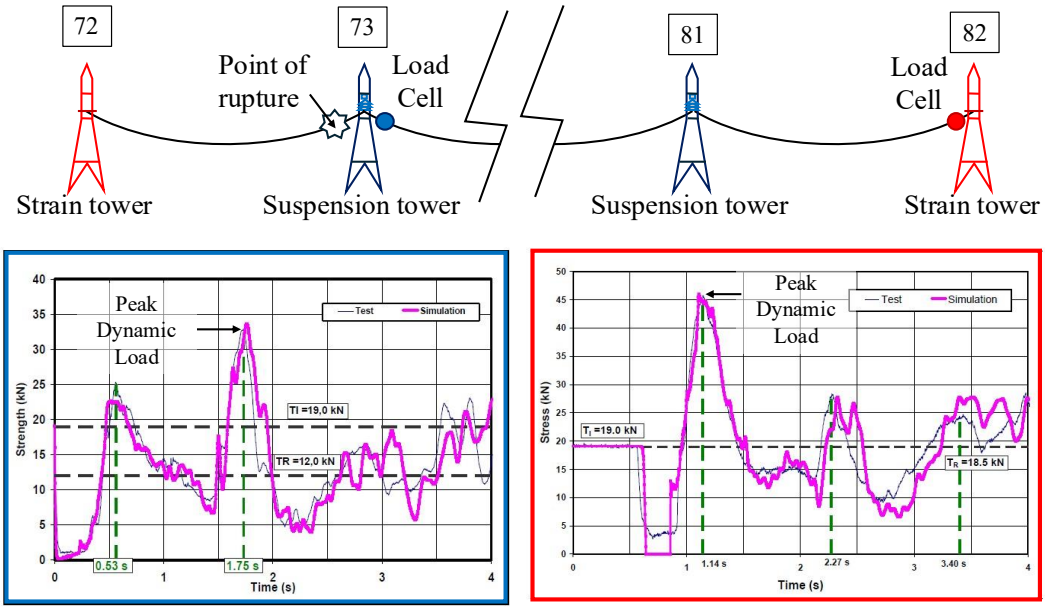

Figure 1: Load at suspension (73) and strain support (82) following a broken wire event. Test and simulation results adapted from Vicent Pierre (2004)

Building upon this foundation, the present paper focuses specifically on conductor failure events. Our work introduces a newly calibrated finite element model and validates it against experimental results from the EPRI Dynamic Impact Test Line, resulting in improved accuracy for predicting dynamic response. Key model parameters such as conductor type, insulator length, suspension and strain structure stiffness, span lengths, and initial tensions are systematically varied to assess their influence on system behavior. Initial analyses are performed using a single-span model, followed by a multi-span approach.

The dynamic load factor (DLF), which provides a measure of the peak dynamic load, is calculated by identifying the single highest peak tension observed, regardless of when it occurs, and comparing it to the intact or installed wire tension. Specifically, the DLF is defined as the ratio of the maximum peak tension recorded in the suspension or strain loading to the tension

present in the undamaged conductor (Eq. (1)).

$$DLF = \frac{\text{Peak Tension}}{\text{Intact Wire Tension}} \tag{1}$$

Given the significant cost and complexity of physical testing, the Finite Element Method (FEM) approach presented here using ADINA (2024) provides a valuable and efficient means to explore a wide range of scenarios that are difficult to assess experimentally. The modeling process is further facilitated through automated pre- and post-processing Python routines. This enables comprehensive sensitivity analyses and deeper understanding of the effects of key variables in transmission line dynamics under conductor rupture conditions. The opportunity to perform this research is made possible thanks to the support and resources provided by EPRI and the full set of analyses are referenced in EPRI (2024).

2 VARIABLES AFFECTING DYNAMIC IMPACT

The main variables affecting the dynamic impact are shown in Figure 2 and are: conductor properties, insulator length, suspension stiffness, strain stiffness, span length, installed tension ($\boldsymbol{H}$), conductor weight ($\boldsymbol{w_u}$), catenary constant (**a**) and number of suspension structures.

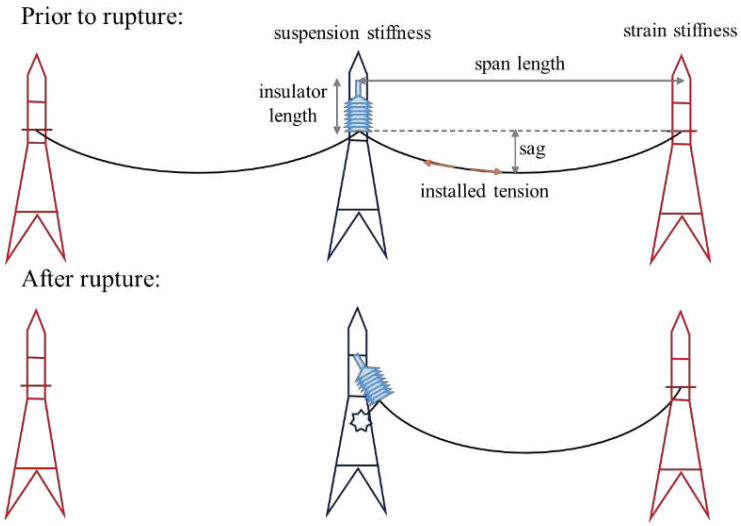

Figure 2: Main variables affecting dynamic impact

The catenary constant is defined in Eq. (2).

$$a = \frac{H}{w_u} \tag{2}$$

Eq. (3) describes the catenary curve of the conductor, where the vertical position (**y**) at any point (**x**) along the span can be found as a function of the catenary constant a. The sag occurs at the mid-span and is defined as the difference between the height at the end points and the lowest point in the middle of the span.

$$y = a[\cosh\left(\frac{x}{a}\right) - 1] \tag{3}$$

3 CONDUCTOR AND INSULATOR PROPERTIES

The properties of a Drake Aluminum-Conductor Steel-Reinforced (ACSR) cable are presented in Table 1. This paper focuses solely on analyzing the Drake ACSR conductor; however, the FEM model can be readily modified to simulate other types, such as the Merlin

or Chukar ACSR conductors, which were modeled but not presented in this paper. Insulator properties, which are also part of the FEM, are also indicated in Table 1. The main characteristics of the Drake cable are that the steel core provides high tensile strength, allowing for longer spans and higher voltage transmission, while the aluminum strands carry the electrical current, taking advantage of aluminum's good conductivity.

Description	Drake ACSR	Insulator
Size (kcmil)	795	-
Stranding (Alum/Steel)	26/7	-
% Steel by weight	31.4	-
Rated Tensile Strength (kN)	140.1	-
Total area (mm²)	468.6	201.1
Diameter (mm)	28.1	16
Unit mass (kg/m)	1.63	0.40
Density (kg/m³)	3471	2000
Final modulus of elasticity (GPa)	69.64	37

Table 1: Properties of the Drake ACSR conductor and insulator structure used in the proposed FEM model

3.1 ACSR Damping

The damping of the conductor is important to the dynamic analysis as it affects the magnitude of the calculated peak load. Damping of transmission conductors includes internal damping and aerodynamic damping. Internal damping is a combination of hysteretic damping within the individual cable strands and damping due to the sliding friction between strands as they move past one another during cable movement. Mathematically, this can be divided into two parts: axial damping that takes place due to changes in the conductor tension, and lateral damping due to bending of the conductor. The critical axial viscous damping constant (C_{cr}) for a rod is given in Eq. (4), where A, E, and m_u are the total area, modulus of elasticity, and unit mass of the rod. In this case, the area of the Drake conductor is equal to the summed area of the internal aluminum and steel conductors, and thus only one E (provided by the manufacturer) is considered, which is constant. An internal damping of 0.5% of the critical axial damping is used (see Section 4.3). Note that the critical damping constant is independent of the length of the rod.

$$C_{cr} = 2\sqrt{A\,E\,m_u} \tag{4}$$

Additionally, aerodynamic damping must be considered, which is due to the motion of the conductor through the air. ADINA (2024) allows for modeling the aerodynamic damping directly. Eq. (5) shows the calculation for aerodynamic damping:

$$F_d = \frac{1}{2}\rho_{air} V_r^2 C_d A_p \tag{5}$$

where F_d is the damping force, ρ_{air} is the air density, V_r is the velocity relative to the air, C_d is the drag coefficient, and A_p is the projected area of the conductor. C_d depends on the Reynolds number and a C_d of 1.25 is used based on the calibration shown in Section 4.3.

Although the aerodynamic damping should be applied normal to the direction of movement, this would be more difficult to model in ADINA (2024). Instead, the aerodynamic damping is applied to the vertical motion of the conductor using the initial horizontal projected area. This is a simplified approach, where the damping force is proportional to the vertical velocity of the conductor relative to still air, rather than modelling the fluid-structure interaction.

4 FINITE ELEMENT MODEL

The finite element model was developed in ADINA (2024), where truss, spring, and damper elements were used according to Peabody (2003). Figure 3 and Figure 4 show the layout of the 2D conductor model with damping and the 2D structure model, respectively. For this study, all finite element models were constructed as planar (2D) systems, representing the conductors and supporting structures in a vertical plane.

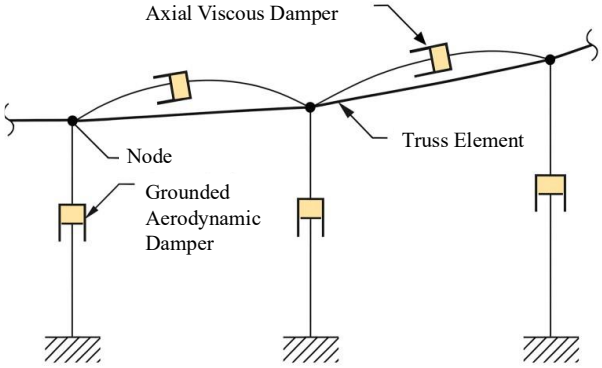

Figure 3: Conductor model with damping adapted from Peabody (2003)

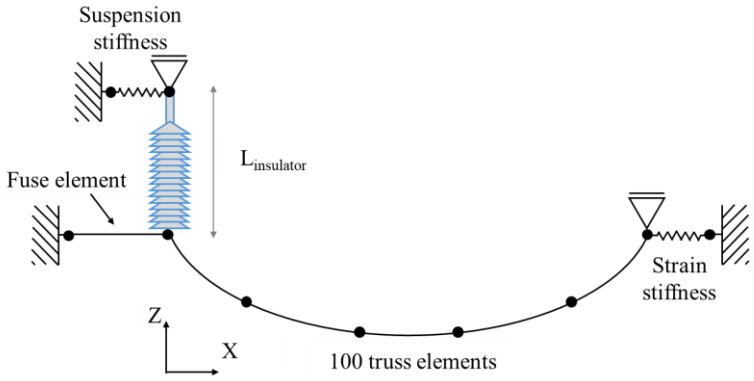

Figure 4: Structure model adapted from Peabody (2003)

The conductor is represented by tension-only pin-connected truss elements with nonlinear elastic material properties to capture inability to carry compression (i.e., no stiffness in compression). A fuse element, which is used to hold the conductor in tension (see Section 4.2), is modeled as a truss element. For the suspension and strain truss elements, an elastic material is used with the modulus of elasticity adjusted to achieve the required stiffness based on unit length and area, represented as springs in Figure 4. The suspension insulator is positioned at the end of the tower spring, modeled as a truss element with properties corresponding to the fiberglass rods commonly used in non-ceramic insulators. Note that the following modeling parameters were used: large displacement analysis, full Newton–Raphson iteration with line search, and tight convergence criteria for energy (10E-8) and displacement (10E-6) according to Bathe (1996). While the structural analysis employs large displacement formulations to capture geometric nonlinearities during dynamic events, the aerodynamic damping model is linearized and applied in the vertical direction only. This simplification was adopted to maintain computational efficiency and is consistent with previous validated approaches Peabody (2003).

The entire modeling process was fully automated using a Python script, which allows the user to define all relevant parameters during pre-processing, execute the ADINA Structures

solver, and post-process the results to obtain the loadings at desired structural locations. The modeling workflow consists of two main stages, which are described in detail in the following subsections.

4.1 Static stage

First, a static analysis is performed in which the conductor coordinates are calculated based on the specified horizontal tension and unit weight using the catenary equation described in Eq. (3). A mass proportional load equal to the acceleration due to gravity is applied. Initial strains for the suspension and strain structures are modelled by dividing the initial tension of the conductor by each structure's area and modulus of elasticity. The static analysis is performed for a time period of 1 s and the results are saved in an ADINA restart file. The static stage gives the resulting shape of the conductor in equilibrium between its own weight and an initial tension, which is used as the basis for the dynamic analysis.

4.2 Dynamic stage

The beginning of the dynamic analysis starts at 1.10 s, at which point the fuse element is erased. This follows the recommendation of ADINA (2024) of removing a model element to simulate a breakage. The model is run until 11 s using a time step of 0.1 μs. The dynamic direct integration method is used, restarting from the equilibrium position obtained in the static stage. From this stage, the progression of loading at the suspension, insulator, and strain structures as a function of time is obtained and the DLF calculated.

4.3 Calibration of the model

To calibrate the finite element model, the FEM model was compared to full-scale tests completed at the EPRI installation. The full-scale tests were completed at the Dynamic Impact Test Line at the EPRI High Voltage Laboratory in Massachusetts, USA shown in Figure 5.

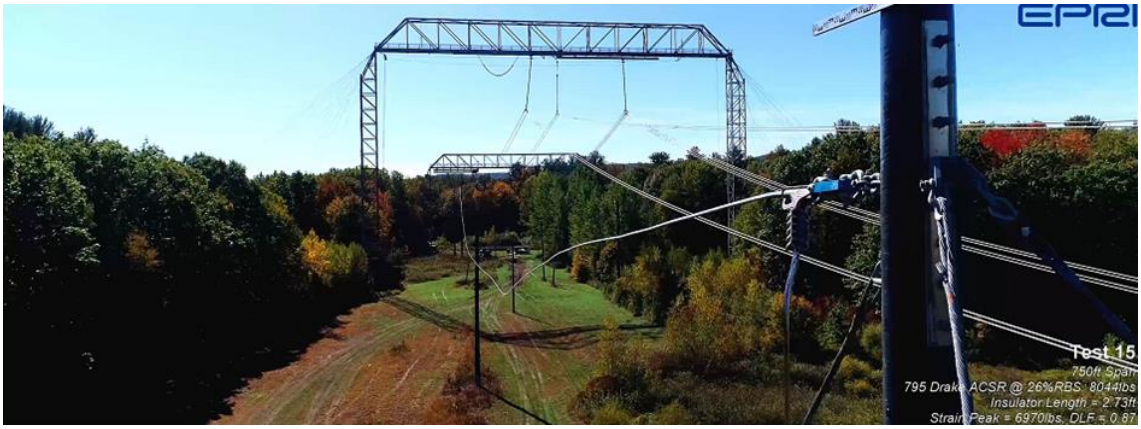

Figure 5: Dynamic Impact Test Line at the EPRI High Voltage Laboratory

Two full-scale tests using the Drake ACSR conductor are described in this paper following the properties shown in Table 2.

Full-scale test and FEM modeling results are shown in Figure 6 and Figure 7. Note that for the results shown, the following parameters were calibrated: a converged timestep of 0.1 μs; a filtering frequency of 10 Hz with a moving filter; 100 truss elements, which allowed for convergence without excessive computation times; an internal damping coefficient of $0.005C_{cr}$; and a coefficient C_d of 1.25 and aerodynamic drag exponent XN of 2. These parameters were

found through a series of sensitivity tests, resulting in calibrated parameters that could be used for other trials.

The ADINA results show a high agreement with the full-scale results provided by EPRI for each structure in Test 1 and the strain structure in Test 2. For Test 2, the DLF at the suspension structure between the simulated and real data differs by 23%. However, this is likely due to filtering the ADINA data. High frequency content observed in the ADINA simulations was not present in the experimental data, which is why filtering was applied to the numerical outputs following Peabody (2003). Therefore, it is likely that a higher degree of matching is possible depending on the type of filter used. Numerical filtering, specifically a 10 Hz filter, was applied to the FEM simulation results to match the frequency bandwidth of the test data. While further model refinement could potentially reduce the need for filtering, the filter provided an efficient and practical solution for accurate comparison.

	Full-scale test no.	1	2
Line parameters	Span length (ft)	750	750
	Conductor (-)	Drake	Drake
	Weight/unit length (lb/ft)	1.093	1.093
	Catenary constant (ft)	4980	4915
	Insulator length (in)	91.8	94.5
	Suspension stiffness (lb/in)	6856	860
	Strain stiffness (lb/in)	5417	3981
	Installed tension (lbs)	5443	5372
Suspension structure	Peak load (lbs)	6385	7939
	Dynamic load factor (-)	1.16	1.46
Strain structure	Peak load (lbs)	6905	6516
	Dynamic load factor (-)	1.25	1.20

Table 2: Test properties for full-scale tests conducted by EPRI

In general, the response of the structures is consistent with the trends found by Vicent Pierre (2004). The first peak occurs as the suspension insulator is pulled in-line with the conductor as shown in Figure 8.

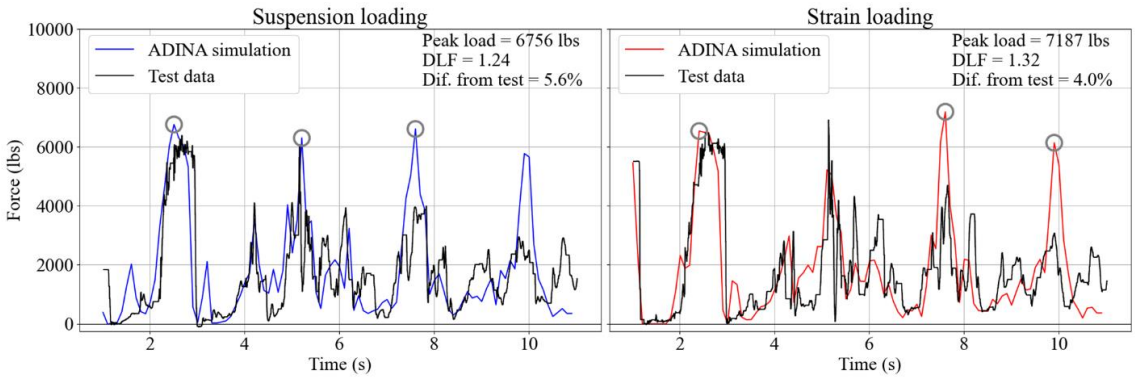

Figure 6: Test 1 – Comparison between ADINA results and full-scale EPRI data for a Drake conductor

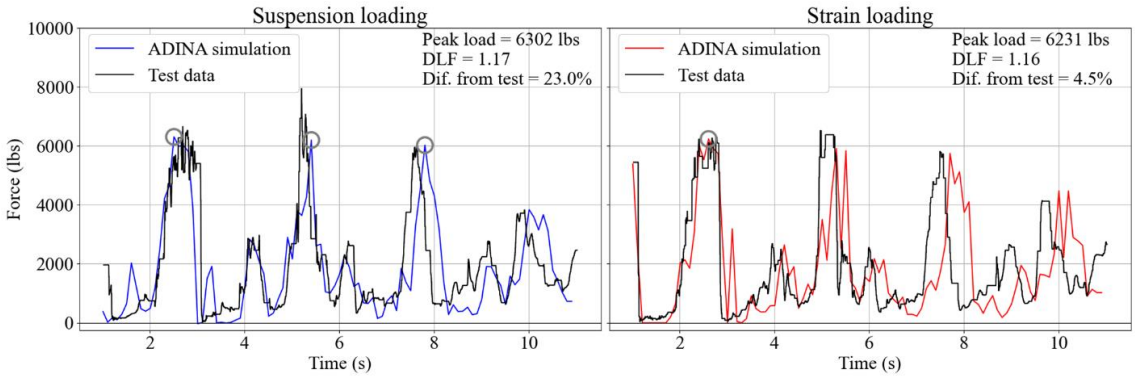

Figure 7: Test 2 – Comparison between ADINA results and full-scale EPRI data for a Drake conductor

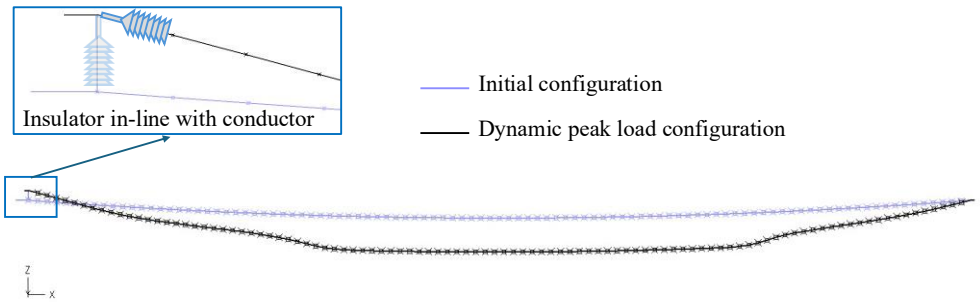

Figure 8: Test 1 – Initial and peak loading configurations. The first load peak occurs when the insulator is in-line with the conductor

5 SUSPENSION STIFFNESS SENTIVITY

After calibration, many sensitivity tests were conducted to analyze trends in DLF vs. conductor properties. In this section, only the results on varying suspension stiffness, with remaining parameters held constant, are shown. Specifically, tests on a 500 ft-long Drake conductor are completed using suspension stiffnesses ranging from 100 to 1000 lb/in. The full set of sensitivities, including those for other conductors, are described in EPRI (2024).

The results for this sensitivity analysis are shown in Figure 9. These results follow an expected trend, where an increase in suspension stiffness results in a higher DLF at both structures. Additional testing was completed by EPRI (2024), which showed that this increase plateaus beyond a suspension stiffness of 1000 lb/in.

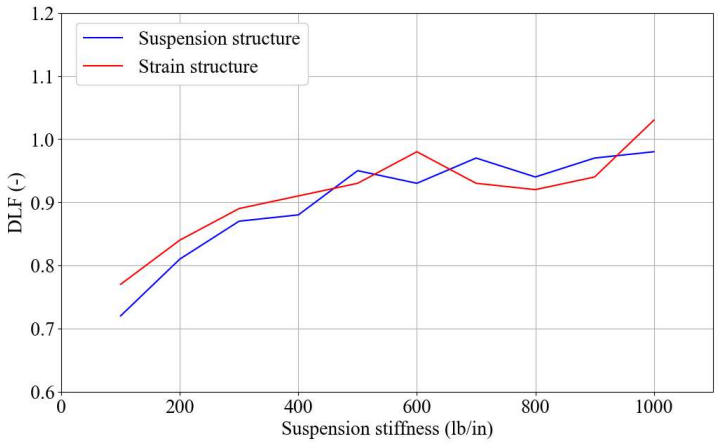

Figure 9: Sensitivity results for a Drake conductor and varying suspension structure stiffness

6 MULTIPLE SPAN ANALYSIS

The previous tests all consider a single-span FEM model. However, it is possible to simulate a multi-span model, i.e., a model containing multiple intermediate suspension structures. Thus, a sensitivity analysis is conducted on the number of intermediate suspension structures following the scheme shown in Figure 10.

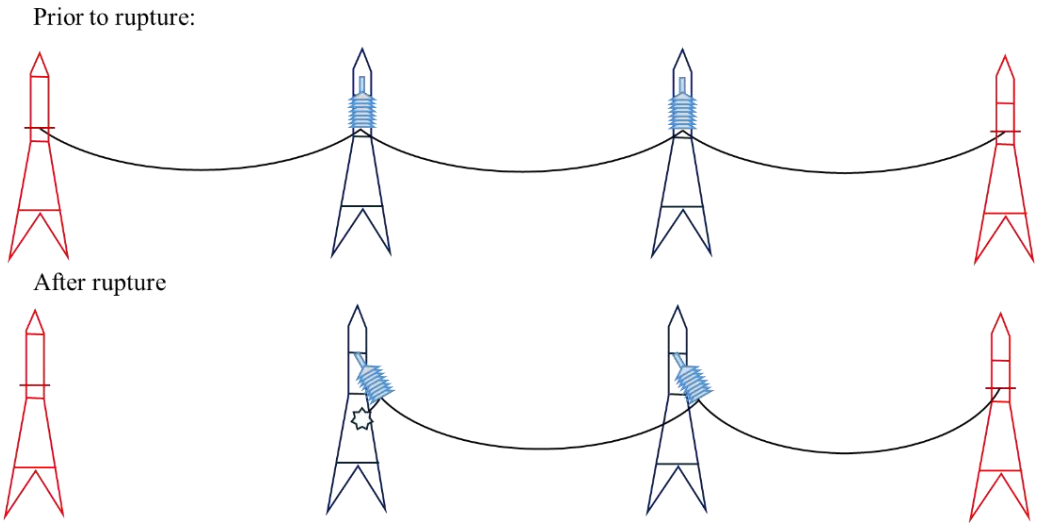

Figure 10: Example of a multi-span model with two intermediate suspension structures

The same parameters as Section 5 are used with a suspension stiffness of 1000 lb/in. However, the number of suspension structures is varied from 1 to 10, with additional tests considering 15 and 20 structures. The results are shown in Figure 11. Note that an increase in the amount of suspension structures generally results in a higher DLF at the strain structure that asymptotes after about 10 suspension structures. However, the results for the initial, or first, suspension structure are less clear. These results are likely complicated by the reflection and stacking of the shockwaves between structures, and thus more study may be required.

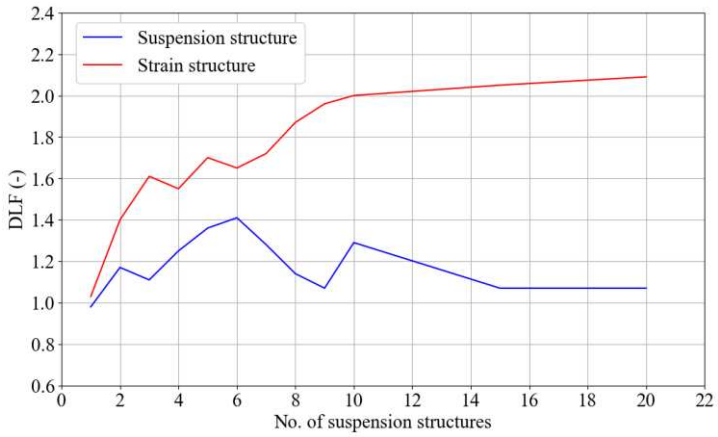

Figure 11: Results of a multi-span sensitivity analysis using a Drake conductor

7 CONCLUSIONS

While conductor failures are rare, broken conductor events can lead to high costs and damages within the energy sector. Therefore, it is important to properly model broken

conductor events to better understand their effect on transmission lines. This study demonstrates that the ADINA (2024) finite element modeling software is an effective tool for simulating the dynamic behavior of broken conductor events, allowing users to model a wide variety of scenarios and perform extensive sensitivity analyses without the need for costly and time-consuming full-scale experimental tests.

To begin, a finite element model is created using typical conductor and transmission tower properties with careful consideration for axial and aerodynamic damping. This model is then calibrated against a full-scale test conducted at the Dynamic Impact Test Line at the EPRI High Voltage Laboratory. This process allows for calibrating various modeling parameters, such as damping coefficients, convergence criteria, and element discretization, which are then used for other broken conductor models.

After calibration, various sensitivity analyses are performed. The first sensitivity analysis is performed on the stiffness of the suspension structure. The results show that, in general, an increase to the suspension structure stiffness results in an increase to the dynamic load factor (DLF), which is a measure of the peak loading in the conductor compared to its initial tension. Additional testing by EPRI (2024) shows that this effect plateaus after a suspension stiffness of about 1000 lb/in, which is the highest stiffness reported in this study. Additionally, a sensitivity analysis was performed on the number of suspension structures. The results show that as the number of intermediate suspension structures increases, the DLF of the strain structure increases with a plateau after about 10 structures. However, the results are less clear when reviewing the DLF of the initial suspension structure, which is likely due to the reflection and stacking of the shockwaves within the conductor. Thus, more study is needed to understand the effects of a multi-span configuration.

The results of this study confirm that ADINA (2024) is well suited for detailed dynamic modeling of transmission lines under broken conductor conditions. With the addition of an automated workflow, many simulations can be performed quickly and accurately, providing insight into various parameters' effects on DLF. It is important to note that certain factors were not included in the current study, such as the tower structures' natural frequencies, additional types of damping, or foundation stiffness. Including these aspects in future studies may further enhance the applicability of the numerical model and improve understanding of broken conductor events.

ACKNOWLEDGMENTS

We would like to thank EPRI and Jean-Pierre Marais for their support and sponsorship of this research. For inquiries regarding the research initiative, please contact EPRI.

REFERENCES

ADINA R&D Inc. *Automatic Dynamic Incremental Nonlinear Analysis (ADINA), Theory and Modeling Guide: Volume I*. Bentley Systems, Inc, 2024.

Alan B. Peabody. *Modeling the EPRI-Wisconsin Power and Light Broken Wire Tests*. *Structural Engineering Series*, 2003.

Bathe, K.-J. *Finite Element Procedures*. Upper Saddle River, NJ: Prentice Hall, 1996

Practical Determination of Dynamic Load Impact Factors: 2024 *Update –Results from Dynamic Impact Test Line. EPRI*, Palo Alto, CA: 2024. 3002029585.

Vincent Pierre, et al. *Testing and numerical simulation of overhead transmission line dynamics under component failure conditions*. Cigré. Session, 2004.